



## 28 1 INTRODUCTION

29 Accurate monitoring of water and vegetation stress is now of prominent global concern and it is  
30 regarded as a high priority issue (Petropoulos et al., 2016). Much emphasis is placed on the  
31 accurate monitoring of the effects of climate change on water and vegetation, particularly for  
32 communities located in the Mediterranean region having water scarce ecosystems (Amri et al.,  
33 2014). Thus, studies on the partitioning of incoming energy into heat and water fluxes is crucial  
34 in understanding the mechanism of climate change. The terrestrial boundary layer and its  
35 vegetation play a critical role in regulating the partitioning of incoming energy (into Latent (LE),  
36 Sensible (H) and Ground (G) heat fluxes), having an effect in photosynthesis and the energy and  
37 water vapour cycles (Prentice et al., 2014).

38 Research on improving our understanding of the representation of land atmosphere interactions  
39 has led to the development and exploration of a wide variety of different modelling schemes. A  
40 number of Land Surface Models (LSMs) for assessing the contribution of different variables  
41 associated with land surface interaction at various degrees of complexities have been developed  
42 since the 1970's. Since then, LSMs have evolved from simple bucket models without vegetation  
43 consideration (e.g. Manabe, 1969) into contemporary versions with credibly detailed  
44 representations of the exchanges of energy, water and CO<sub>2</sub> in the soil-vegetation-atmosphere  
45 continuum. Among various forms of LSMs, Soil Vegetation Atmosphere Transfer (SVAT) models  
46 are increasingly gaining recognition in land surface processes and Earth's system component  
47 studies (Ireland et al., 2015). SVATs are mathematical representations of vertical 'views' of the  
48 physical mechanisms controlling energy and mass transfers in the soil -vegetation-atmosphere  
49 continuum. Those models are able to provide deterministic estimates of the time course of soil  
50 and vegetation state variables at time-steps compatible with the dynamics of atmospheric  
51 processes. Fine temporal resolution (often <1 hour) of SVAT models allows simulations to be in  
52 satisfactory agreement with the timescale of the physical process being simulated.

53 Developed by Carlson and Boland (1978), SimSphere is a SVAT model that simulates and  
54 enhances our understanding of boundary layer processes and is being extensively used as a  
55 research, educational and training tool within several universities worldwide. SimSphere these  
56 days has gained a lot of popularity as an extensive tool being synergistically used with Earth  
57 Observation (EO) data due to its ability to provide spatio-temporal estimates of  
58 evapotranspiration (ET) rates and surface soil moisture. Most of these investigations have been  
59 based around the implementation of a data assimilation technique termed the "triangle"  
60 (Petropoulos & Carlson, 2011). Variants of this technique are currently investigated by different  
61 Space Agencies for developing related operational products (Chauhan et al., 2003; Piles et al.,  
62 2011; Piles et al., 2016). A series of SA experiments have already been conducted on SimSphere  
63 (Petropoulos et al., 2009b; Petropoulos et al., 2013a-c; 2014). Those studies provided for the first  
64 time independent evidence to enhance our understanding of the model's behaviour, coherence  
65 and correspondence to that it has been built to simulate (Petropoulos et al., 2009a; Petropoulos  
66 et al., 2013a-c; 2014). However, SimSphere validation has previously only been performed over a  
67 very small range of land use/cover types (e.g. Todhunter and Terjung, 1987; Ross and Oke, 1988;  
68 Petropoulos et al., 2015). Given its current global expansion, such a comprehensive validation of  
69 it is both timely and of fundamental importance to further establishes the model's structure,  
70 coherence and representativeness in terms of its ability to realistically represent Earth's land  
71 surface interactions.

72 In light of the above, this study's objective has been to investigate the ability and applicability of  
73 SimSphere to simulate a series of significant variables characterising land surface interactions

74 and specifically: Net Radiation ( $R_{net}$ ), Latent Heat (LE) and Sensible Heat (H). For this, purpose,  
75 *in-situ* measurements a total of 70 days selected from 7 model European ecosystems sites  
76 representative of different conditions the CarboEurope monitoring network in Europe have been  
77 used to validate the model's output.

78

## 79 **2 MODEL FORMULATION**

80 SimSphere simulates the land-atmosphere exchanges taking place in a vertical column that  
81 extends from the root zone below the soil surface up to a level well above the surface canopy, the  
82 top of the surface mixing layer. SimSphere was considerably modified to its current state by  
83 Gillies et al. (1997) and later by Petropoulos et al. (2013d) and Anagnostopoulos et al., (in press).  
84 It is currently maintained and freely distributed by Aberystwyth University, United Kingdom  
85 (<http://www.aber.ac.uk/simsphere>). A detailed description of its architecture can be found in  
86 Gillies (1993) and an overview on its use can be found in Petropoulos et al., (2009 b).

87 Briefly, SimSphere is a 1-dimensional two-source SVAT model with a plant component (input  
88 parameters shown in **Table 1**). The model structure is an integrated form of 3 major components  
89 namely the *physical*, *vertical* and *horizontal* layers. The *physical* component determines the  
90 microclimate in the model and primarily takes account of the available radiant energy radiant  
91 energy reaching the surface in clear sky condition or the plant canopy. The component is  
92 calculated as a function of sun and Earth geometry, atmospheric transmission factors for  
93 scattering and absorption, the atmospheric and surface emissivity's and surface (including soil  
94 and plant) albedos. The *vertical structure* components (Fig. 1, right), effectively corresponds to  
95 the components of the Planetary Boundary Layer (PBL) that are divided into three layers - a  
96 surface mixing layer, a surface of constant flux layer and a surface vegetation or bare soil layer.  
97 Vegetation and soil fluxes mix at the top of the vegetation canopy. Their relative weights depend  
98 on the fractional vegetation cover (FVC), specified as an input to the model. The soil hydraulic  
99 parameters are prescribed from the Clapp and Hornberger (1978) classification. The soil surface  
100 turbulent fluxes are determined following the Monin and Obukhov (1954) similarity theory which  
101 takes into account atmospheric stability. The Atmospheric Boundary Layer (ABL) conditions are  
102 provided by a one dimensional ABL model.

103 SimSphere simulates the processes and the interaction between soil, plant and atmosphere layers  
104 over a 24-hour cycle. The cycle runs at a chosen time step, starting generally from the early  
105 morning (at 06: 00 am local time) to monitor the continuously evolving interaction between the  
106 input layers. A number of input parameters are required to parameterise the model, categorised  
107 into 7 defined groups (**Table 1**) and the model provides predictions as a function of time for a  
108 total of more than 30 variables (**Table 1**).

109

110 **Figure 1:** (Left) *The three facets of SimSphere Architecture*, (Right) *different layers represented*  
111 *within SimSphere's vertical domain*

## 112 **3 MATERIALS AND METHODS**

113 **Figure 2** provides details of the methodology followed to parameterise and validate SimSphere  
114 targeted outputs, whereas the major steps involved in this process are outlined below.

### 115 **3.1 *In-situ* Datasets Collection**

116 This study evaluates the ability of SimSphere Soil Vegetation Atmosphere Transfer (SVAT) model  
117 in providing diurnal estimates of key variables characterising water and energy balance at 7  
118 CarboEurope sites, part of a larger observational network, FLUXNET (Baldocchi et al., 2001). The  
119 sites used in our study were selected as representative of different ecosystem types (see **Table**  
120 **2**). *In-situ* data for selected sites were acquired from the European Fluxes database Cluster  
121 (<http://gaia.agraria.unitus.it/>) for the year 2011. In particular Level 2 data were obtained across  
122 all selected sites for consistency. This product includes the originally acquired *in-situ*  
123 measurements from which only the removal of erroneous data caused by obvious  
124 instrumentation error were undertaken. In addition, atmospheric profile (i.e. radiosonde) data as  
125 atmospheric temperature profile, dew point temperature, wind direction, wind speed and  
126 atmospheric pressure were obtained for each site/day from the University of Wyoming  
127 (<http://weather.uwyo.edu/upperair/sounding.html>).

128

129 **Figure 2:** Overall methodology of SimSphere validation followed in this study

130 Initially, for each site, cloudy days were identified and were subsequently excluded from further  
131 analysis. Identification of cloudy days was carried out using diurnal incoming global solar  
132 radiation ( $R_g$ ) observations. As cloud-free days were flagged as those having smoothly  
133 symmetrical  $R_g$  curves and as cloudy those having an asymmetrical one (Carlson et al., 1991).  
134 Subsequently, energy balance closure (EBC) for those clouds free days only was evaluated. EBC is  
135 believed to be the most relevant energy measurement tool as its magnitude depends on more  
136 accurate entities such as Latent Heat (LE) and Sensible Heat (H) and not on other scalar fluxes  
137 such as  $CO_2$  (Wilson et al., 2002; Foken et al., 2006). EBC was evaluated principally by calculating  
138 the linear regression coefficients (slope and intercept) as well as the coefficient of determination  
139 ( $R^2$ ) from the ordinary least squares (OLS) relationship between the half-hourly estimates of the  
140 dependent flux variables (LE+H) and the independently derived available energy ( $R_{net}-G-S$ ). In  
141 addition, the Energy Balance Ratio (EBR) was also computed by cumulatively summing  $R_{net}-G-S$   
142 and LE+H from the 30-min mean average surface energy flux components, and then rationing  
143 each of the cumulative sums as follows (Liu et al., 2006):

144 
$$EBR = \frac{\sum (LE + H)}{\sum (R_{net} - G - S)} \quad (1)$$

145 where LE is the Latent Heat, H is the Sensible Heat,  $R_{net}$  is the net radiation, G is the heat  
146 flux into the soil, and S is the rate of change of heat storage (air and biomass). This index  
147 ranges generally from zero to one, with values closer to one highlighting a satisfactory  
148 diurnal energy closure, indicating a good quality of *in-situ* measurements.

149 All days with low EBC (i.e.  $EBR < 0.750$ , slope < 0.85,  $R^2 < 0.930$ ) were excluded from further  
150 analysis. Further constraints were applied to calibrate the selected data quality with the *in-situ*  
151 data quality which was performed over several steps. Secondly, atmospherically stable  
152 conditions, such as low wind speeds and small available energy, were selected for the evaluation  
153 simulation days (Maayar et al., 2001). Such conditions were identified during evaluation of the *in-*  
154 *situ* dataset, where direct measurements of wind speed and energy flux amplitude and diurnal  
155 trend were used as indicators of atmospherically stable conditions. In total a set of 70 non-  
156 consecutive days from the 7 CarboEurope sites were identified as being suitable to include in the  
157 model verification.

158

## 159 3.2 SimSphere Parameterisation & Implementation

160 SimSphere parameterisation was carried out at the measurement scale of the flux tower  
161 observations, i.e. the area of the possible measurement fetch around which the tower is built and  
162 the footprint of the turbulent flux measurements, representing an area of  $\sim 1\text{km}^2$  for the test sites  
163 as they are relatively homogeneous. On this basis, SimSphere was parameterised to the daily  
164 conditions existent at the flux tower for each of the selected days.

165 For each day the model was parameterised to the daily existing conditions at the flux tower up to  
166 a height of 54,000ft. Initial conditions for air temperature, dew point temperature, atmospheric  
167 pressure, wind speed and direction were used within the 'Wind Sounding' and 'Water Vapour  
168 Sounding' components of the model. These details were data were acquired from the publically  
169 available University of Wyoming database, and were collected at 6:00am GMT to correspond to  
170 the model's initialisation. Ancillary information on vegetation and soil parameters (e.g. Leaf area  
171 index - LAI, FVC, vegetation height, soil type etc.) was also used directly within the model's  
172 initialisation. Such information was acquired in most cases directly from communication with the  
173 principal investigators of each respective site, though in some cases it had to be acquired from  
174 standard literature sources (e.g. Mascart et al., 1991; Carlson et al., 1991). The soil type  
175 parameters were obtained using the soil texture data provided at each CarboEurope test site.  
176 Similarly, this was also the case for the topographical information that was required in model  
177 initialisation. Upon model initialisation, the model was executed for each site/day and the 30'  
178 average value of each of the evaluated parameters per site for the period 0530-2330 hours was  
179 subsequently exported in SPSS for comparisons against the corresponding *in-situ* data.

180

## 181 3.4 Validation

182 To analyse the correlation of the model simulated values to the observed, a series of statistical  
183 approaches based on the results of many previous similar studies (e.g. Giertz et al., 2006;  
184 Marshall et al., 2013). Those included were root mean square difference [RMSD], the linear  
185 regression fit model coefficient determination [ $R^2$ ], the Bias or Mean Bias Error [MBE], the  
186 Scatter or mean standard deviation [MSD], the mean absolute error [MAE] and the NASH index,  
187 tabulated in **Table 3**. MSD was employed to express the model precision and ultimately for the  
188 correction of non- systematic error. All statistical matrices were computed from the comparative  
189 analysis of the two datasets for each day of comparison at 30' intervals. The same set of statistical  
190 metrics was performed on the dataset for each of the CarboEurope sites for each of the selected  
191 days.

192

## 193 4 RESULTS

### 194 4.1 Net Radiation ( $R_{\text{net}}$ ) flux

195 The results of the analysis between SimSphere predicted and *in-situ* Net radiation measurement  
196 are summarised in **Table 4**. Furthermore, **Figure 3a** illustrates the agreement between the *in-*  
197 *situ* and the predicted  $R_{\text{net}}$  for all days of comparisons from all experimental sites. For most of the  
198 compared days diurnal variation of the simulated  $R_{\text{net}}$  in general was found in close  
199 correspondence with the observed  $R_{\text{net}}$  both in shape and magnitude (although results are not  
200 shown here for brevity).

201 In overall,  $R_{\text{net}}$  simulated by SimSphere was found to be reasonably accurate with an average  
202 RMSD of  $64.65 \text{ Wm}^{-2}$  and a correlation coefficient of 0.96. A minor underestimation of the *in-situ*

203 data was evident for all sites and days combined (MBE =  $-2.07 \text{ Wm}^{-2}$ ), though overall  $R_{\text{net}}$  showed  
204 a significant range of agreement, with RMSD ranging from 24.38 to 98.26  $\text{Wm}^{-2}$  between the  
205 validation days. Interestingly, a noticeable trend between extended observation time period and  
206 simulation accuracy was observed within a number of test sites. Also, notably, there were  
207 increased periods within a number of test sites where simulation accuracy was found increasing  
208 depending on the period in which the simulation days were located. Such trends were observed  
209 for the IT\_Ro3 cropland site, where error ranges decreased for the period between late April  
210 (21/04/2011) and late August (28/08/2011), before increasing in early September  
211 (09/09/2011). However, the periods of increased accuracy varied on a per site basis and were  
212 only prevalent within the olive plantation (ES\_Lju), grassland (IT\_Mbo), cropland (IT\_Ro3) and  
213 deciduous broadleaf forest (IT\_Col) sites. Daily  $R^2$  values exhibited less variance with generally  
214 more comparable ranges (0.909 – 0.998) between all the study days, suggesting a satisfactory  
215 agreement between both datasets, also illustrated by the distribution of the points around the 1:1  
216 line in **Figure 3a**. This was also reflected within the NASH index values reported (0.897 – 0.999).

217 When averaged per site, RMSD showed significantly less variance, exhibiting a range from  
218  $55.86 \text{ Wm}^{-2}$  (IT\_Lav) to  $68.49 \text{ Wm}^{-2}$  (FR\_Pue). This trend was also reflected by lower variance in  
219 correlation coefficients ( $R^2 = 0.936 - 0.970$ ) and NASH index values (0.943 – 0.981) for the per  
220 site averages. The evergreen needle-leaf forest site, IT\_Lav, consistently demonstrated the  
221 highest model performance in simulating  $R_{\text{net}}$  with an RMSD value of  $55.86 \text{ Wm}^{-2}$ , that being  $8.79$   
222  $\text{Wm}^{-2}$  lower than the overall average. MBE between sites showed significant variability, ranging  
223 from a moderate underestimation of the *in-situ* measurements over the evergreen broadleaf  
224 forest site ( $-15.99 \text{ Wm}^{-2}$ ), to a moderate overestimation within the shrubland site ( $15.02 \text{ Wm}^{-2}$ ).  
225 All in all, SimSphere was able to reproduce  $R_{\text{net}}$  reasonably well in terms of both amplitude and  
226 trend. Indeed, this is reflected in the low MSD values of all sites ( $55.01 - 68.03 \text{ Wm}^{-2}$ ), particularly  
227 so at sites such as IT\_Lav ( $55.01 \text{ Wm}^{-2}$ ) and ES\_Agu ( $60.92 \text{ Wm}^{-2}$ ).

228

229 **Figure 3:** Comparisons of predicted and observed a)  $R_{\text{net}}$  fluxes ( $\text{Wm}^{-2}$ ), b) LE fluxes ( $\text{Wm}^{-2}$ ), c) H  
230 fluxes ( $\text{Wm}^{-2}$ ), and d)  $T_{\text{air}}$  at 50m ( $^{\circ}\text{C}$ )

231

## 232 **4.2 Latent Heat (LE) flux**

233 SimSphere simulated LE flux and the CarboEurope LE measurement for all combined days  
234 exhibited an overall average RMSD error of  $62.75 \text{ Wm}^{-2}$  and a correlation coefficient value of  
235 0.542 respectively (**Table 5**). Although RMSD for the LE output showed a better agreement in  
236 comparison to the  $R_{\text{net}}$  output (section 4.1),  $R^2$  was significantly lower (a decrease of 0.408). As  
237 can be seen from **Figure 3b**, the distribution of points shows an increased dispersion from the  
238 1:1 line in comparison to the  $R_{\text{net}}$  output. There was also an apparent overestimation of the *in-situ*  
239 measurements by the model for the LE flux (MBE =  $15.78 \text{ Wm}^{-2}$ ).  $R^2$  values varied significantly  
240 between all simulation days from 0.020 – 0.961, suggesting notable discrepancies between the  
241 predictions and observations. Additionally, daily RMSD values also varied significantly, reflecting  
242 the trends observed in the  $R^2$  statistics. RMSD varied from  $22.08 \text{ Wm}^{-2}$  to  $86.45 \text{ Wm}^{-2}$  between all  
243 days of simulation. When analysed on a site by site basis, average RMSD exhibited comparable  
244 ranges to those reported for the individual simulation days, with RMSD varying from  $37.25 \text{ Wm}^{-2}$   
245 (ES\_Agu - Shrubland) to  $75.36 \text{ Wm}^{-2}$  (IT\_Col, deciduous broadleaf forest). On a per site basis,  
246 ES\_Agu shrubland site consistently demonstrated above average correlation to the *in-situ*  
247 measurements with the lowest RMSD and MAE values of all sites,  $37.25 \text{ Wm}^{-2}$  and  $25.58 \text{ Wm}^{-2}$   
248 respectively. Lowest agreement between the LE fluxes predicted from SimSphere and those from

249 the *in-situ* measurements was in the IT\_Col deciduous broadleaf forest site (RMSD = 75.36 Wm<sup>-2</sup>,  
250 MAE = 55.86 Wm<sup>-2</sup>) and IT\_Mbo grasslands site (RMSD = 74.66 Wm<sup>-2</sup>, MAE = 52.87 Wm<sup>-2</sup>)  
251 respectively. On the whole, SimSphere was consistent in terms of its ability to reproduce *in-situ*  
252 LE fluxes, with low MSD values across most sites. Yet, the IT\_Mbo (grassland) and IT\_Ro3  
253 (cropland) sites exhibited the largest MSD of 74.58 Wm<sup>-2</sup> and 68.48 Wm<sup>-2</sup> respectively, an  
254 increase of 15.64 Wm<sup>-2</sup> and 9.54 Wm<sup>-2</sup> on the overall average suggesting a weaker systematic  
255 replication of LE fluxes over those sites (**Table 5**). There was a systematic overestimation of LE  
256 for the majority of sites. Exceptions were only the IT\_Mbo and IT\_Ro3 sites, exhibiting a small  
257 average underestimation (MBE) of -3.45 Wm<sup>-2</sup> and -0.87 Wm<sup>-2</sup> respectively. Interestingly, both  
258 broad-leaf forest sites, IT\_Col (deciduous broad-leaf forest) and FR\_Pue (evergreen broad-leaf  
259 forest), showed the highest overestimation of LE fluxes with moderately high MBE values of  
260 33.67 Wm<sup>2</sup> and 37.56 Wm<sup>-2</sup> respectively.

261

### 262 4.3 Sensible Heat (H) flux

263 Concerning the H fluxes, results showed high performance of the model in simulating values for  
264 H fluxes with an average RMSD of RMSD of 55.36 Wm<sup>-2</sup> and an R<sup>2</sup> value of 0.83 ( **Figure 3c** ,  
265 **Table 6**). A significant improvement in the accuracy of the simulation of the model output in  
266 comparison to both the R<sub>net</sub> and LE was evident. H flux results exhibited a decrease in overall  
267 RMSD of 9.29 Wm<sup>-2</sup> and 7.39 Wm<sup>-2</sup> respectively. Similar trends were also evident in both the MBE  
268 (-0.08 Wm<sup>-2</sup>) and MSD (53.56 Wm<sup>-2</sup>) results for this output, where model performance was better  
269 in comparison to both the R<sub>net</sub> and LE outputs. Although with regards to R<sup>2</sup>, the H flux output  
270 exhibited a minor decrease in correlation (0.83) compared to the R<sub>net</sub> output When examining the  
271 R<sup>2</sup> values for the individual simulation days, there was a significant variation in both correlation  
272 coefficients (R<sup>2</sup> = 0.607 – 0.982) and RMSD (RMSD = 20.03 - 91.07 Wm<sup>-2</sup>). RMSD ranged from  
273 35.50 Wm<sup>-2</sup> (ES\_Agu) to 71.93 Wm<sup>-2</sup> (IT\_Ro3) on a site by site basis. Similarly to LE flux, the  
274 ES\_Agu site reported the highest simulation accuracy (RMSD = 35.50 Wm<sup>-2</sup>, R<sup>2</sup> = 0.944, MBE = -  
275 7.01 Wm<sup>-2</sup>, MSD = 34.80 Wm<sup>-2</sup>). On the contrary, the cropland site IT\_Ro3 consistently reported a  
276 less satisfactory agreement between model prediction and *in-situ* data for H flux. Generally,  
277 SimSphere was often unable to represent the peak of H flux across all sites diurnally; this is  
278 shown by a scatter of peak values as reported in **Figure 3c**. However, the model did neither  
279 consistently overestimate nor underestimate H flux, but produced a range of bias values, with an  
280 average error of -0.08 Wm<sup>-2</sup>. Both the FR\_Pue and ES\_Lju sites showed a predominant  
281 underestimation of H flux at -16.29 Wm<sup>-2</sup> and -17.17 Wm<sup>-2</sup> respectively. Yet, for the IT\_Mbo site, a  
282 moderate overestimation of 16.41 Wm<sup>-2</sup> was reported, suggesting land cover type may be related  
283 to simulation accuracy.

284

## 285 5. DISCUSSION

286 This study presents an evaluation of the SimSphere SVAT model's ability in simulating key  
287 variables characterising Earth's land/surface interaction across a range of European ecosystems.  
288 The model was parameterised for seven sites where a total of 70 days (10 days per site) from the  
289 year 2011 were selected to validate the model's ability to predict Net Radiation (R<sub>net</sub>), Latent  
290 Heat (LE) and Sensible Heat (H). The agreement between the two datasets was evaluated based  
291 on a series of computed statistical metrics using, as reference, *in-situ* data acquired from selected  
292 sites belonging to the CarboEurope monitoring network.

293 In overall, results showed highest agreement of H fluxes to the measured *in-situ* values for all  
294 ecosystems, with an average RMSD of 55.36 Wm<sup>-2</sup>. Predicted LE fluxes and R<sub>net</sub> also agreed well  
295 with the corresponding *in-situ* data with RMSDs of 62.75 Wm<sup>-2</sup> and 64.65 Wm<sup>-2</sup> respectively. Very  
296 high values of the Nash-Sutcliffe efficiency index were also reported for all of the model outputs  
297 evaluated ranging from 0.720 to 0.998, suggesting a very good model representation of the  
298 observations.

299 Those findings are largely in accordance to previous analogous verification studies reported on  
300 the model. For example, Ross and Oke (1988) performed a validation of a previous version of  
301 SimSphere over an urban environment of Vancouver, Canada and reported an acceptable  
302 agreement for H fluxes (average RMSE = 56 Wm<sup>-2</sup>); however significant average error ranges for  
303 LE fluxes (RMSE = 107 Wm<sup>-2</sup>) were also reported in their study. Also, Ross & Oke (1988) noted  
304 that noted that peak values of air temperature diurnal variability should be observed between  
305 1030 – 1430 LST, this is in close correlation to this present study, further appraising SimSphere's  
306 representation of T<sub>air</sub> at 50m. Todhunter and Terjung (1987) further described in detail how  
307 earlier versions of SimSphere dissipated too much of R<sub>net</sub> as LE flux and too little to be lost to H;  
308 the latter correlates well to the Ross and Oke's findings (1988) but also the findings reported  
309 within; where average bias values indicate general net overestimations of LE flux in the order of  
310 15.78 Wm<sup>-2</sup>, compared to the slight average underestimation of H flux at -0.08 Wm<sup>-2</sup>. Yet when  
311 compared with R<sub>net</sub>, the simulated values of LE and H fluxes demonstrated improved model  
312 performance confirmed by the low average RMSD and high overall R<sup>2</sup>. Petropoulos et al. (2015)  
313 in a verification of the model outputs at ecosystems located in the USA and Australia a good  
314 agreement between the model predictions and the *in-situ* measurements (particularly so for the  
315 LE, H, with RMSDs of 39.47 Wm<sup>-2</sup> and 55.06 Wm<sup>-2</sup> respectively).

316 Among all selected experiment sites, the shrubland located at ES\_Agu consistently showed  
317 remarkably low average RMSD in all model outputs assessed, particularly so for LE and H fluxes.  
318 This is likely to be related to the site's characteristics, located within a water limited  
319 environment, where transpiration effects are much lower in amplitude and thus more  
320 predictable, especially given the site's relative homogeneity (Maayar et al., 2001). Akkermans et  
321 al. (2012) stated that underestimations of LE can largely be attributed to overestimations of H.  
322 Such effects were seen most prominently in our validation site ES\_LJU, where a general  
323 underestimation of LE (MBE = -17.17 Wm<sup>-2</sup>) partly contributed to the significant overestimation  
324 of H flux (MBE = 21.09 Wm<sup>-2</sup>). Also, for example Marshall et al. (2013) have suggested that  
325 ecosystems which exhibit increased stand complexity and heterogeneity, such as forested  
326 environments (particularly those with understory vegetation), can have a profound effect on the  
327 overall exchange of mass and energy.

328 In the overall evaluation of the results concerning the model agreement to the *in-situ*,  
329 instrumentation uncertainty in the measured variables themselves should also be partially taken  
330 into account when attempting to explain the disagreement between the simulated and observed  
331 variables (Bellocchi et al., 2010; Oncley et al., 2007; Verbeeck et al., 2009). Generally, R<sub>net</sub>  
332 measurement accuracy error is in the order of 10 %, although, an additional 10%  
333 instrumentation uncertainty should be added due to limited view angle/measuring volume  
334 (especially in the case of rugged terrains) (Baldochi et al., 2001). Typical uncertainty in the LE  
335 and H estimation using the eddy covariance generally varies between 10% to 20% but can be  
336 much higher during periods of low flux magnitude and/or limited turbulent mixing such as at  
337 night (Petropoulos et al. 2013d). For example, Hollinger and Richardson (2005) showed that  
338 uncertainty in flux measurements is inversely proportional to magnitude, the smaller the flux the  
339 greater the relative uncertainty. Also, it should be noted that for some days included in our

340 comparisons, a characteristic of the acquired *in-situ* data for those days was the presence of  
341 many spikes (indicative of very high or very low values). Possible reasons for those spikes could  
342 be instrumental errors, horizontal advection of H<sub>2</sub>O and CO<sub>2</sub>, footprint changes as well as a non-  
343 stationarity of turbulent regime within the atmospheric surface layer (Papale et al., 2006). For  
344 those days, comparisons resulted in a somewhat lower accuracy of model predictions as such  
345 conditions cannot be replicated by the model which assumes homogeneity of vegetation canopy  
346 and ignores horizontal advection.

347 On the whole, despite the occasionally inferior performance of SimSphere in simulating the  
348 examined model outputs for some days/sites, model predictions were found significant in terms  
349 of the representation of the physical and dynamic processes involved in the interactions of the  
350 complex nature of the soil-land-atmosphere system. Moreover, it is important to recognise that  
351 uncertainty is inevitable in any model, which as a model will never be as complex as the reality it  
352 portrays. In this way, SimSphere fulfils its objective as a tool as it identifies the expected trends  
353 and patterns of change, if not always the magnitudes.

354

## 355 **6. CONCLUDING REMARKS**

356 In this study, key findings from a large scale validation of the SimSphere land biosphere model in  
357 numerous European environments were reported. In total, the model's ability to predict Net  
358 Radiation ( $R_{net}$ ), Latent Heat (LE) and Sensible Heat (H) at 7 ecosystems and for 70 cloud free  
359 days in 2011 was examined. A systematic statistical analysis was employed to assess the  
360 agreement between model predictions and corresponding *in-situ* measurements. To our  
361 knowledge, this is the first study reporting results on the validation of SimSphere's ability in  
362 accurately simulating key variables characterising land surface processes, particularly so in  
363 European ecosystems.

364 In overall, SimSphere was able to predict largely accurately the evaluated parameters for most of  
365 the experimental sites. The evaluation and analysis of a model performance allowed for an  
366 increased understanding of the model's representation. This study results provide further  
367 independent evidence that SimSphere has a high capability of simulating variables associated  
368 with the Earth's energy and water balance. As noted by Verbeeck et al. (2009), discrepancies  
369 found in any validation study should be regarded as a positive step when evaluating model  
370 performance. Such studies can also advance our understanding on the amount of complexity  
371 required for adequate representation of land surface processes and interactions between  
372 different components of our Earth system. Further efforts should be directed towards validating  
373 SimSphere at other ecosystems globally as this will allow assessing its applicability as a  
374 universally applied SVAT model. Moreover, as use of the model is currently being explored  
375 synergistically with EO data, including its possible expansion to a 2D model, it would be of  
376 utmost interest to evaluate the overriding effects of SimSphere predictions to the overall  
377 prediction error derived from such synergistic methods.

## 378 **Acknowledgments**

379 Dr. Petropoulos acknowledges the financial support provided by the European Commission under  
380 the Marie Curie Individual Fellowship project "ENViSIoN-EO". Authors would also like to thank  
381 Ms Daisy Rendall and Ms Thalia Tataris for their positive contributions to data processing and  
382 model implementation. We thank as well the PI's of the CarboEurope network for sharing the  
383 acquired data of their experimental sites.

384

385 **References**

- 386 Akkermans, T., Lauwaet, D., Demuzere, M., Vogel, G., Nouvellon, Y., Ardö, J. and Van Lipzig, N.:  
 387 Validation and comparison of two soil-vegetation-atmosphere transfer models for tropical  
 388 Africa, *J. Geophys. Res-Bioge.* (2005–2012), 117, 2012.
- 389 Amri, R., Zribi, M., Lili-Chabaane, Z., Szczypta, C., Calvet, J. C. and Boulet, G.: FAO-56 Dual Model  
 390 Combined with Multi-Sensor Remote Sensing for Regional Evapotranspiration  
 391 Estimations, *Remote Sens.*, 6, 5387-5406, 2014.
- 392 Anagnostopoulos, V. & Petropoulos, G.P.: A Modernized Version of a 1D Soil Vegetation  
 393 Atmosphere Transfer model for use in Land Surface Interactions Studies. *Environmental*  
 394 *Modelling & Software*, 2017 [in press]
- 395 Baldocchi, D., Falge, E., Gu, L., Olson, R., Hollinger, D., Running, S. and Wofsy, S.: FLUXNET: A  
 396 new tool to study the temporal and spatial variability of ecosystem-scale carbon dioxide,  
 397 water vapour, and energy flux densities, *B. Am. Meteorol. Soc.*, 82, 2415-2434, 2001.
- 398 Bellocchi, G., Rivington, M., Donatelli, M. and Matthews, K.: Validation of biophysical models:  
 399 issues and methodologies. A review, *Agron. Sustain. Dev.*, 30, 109-13. 2010.
- 400 Carlson, T. N. and Boland, F. E.: Analysis of Urban-Rural Canopy Using a Surface Heat  
 401 Flux/Temperature Model, *J. Appl. Meteorol.*, 17, 998-1014, 1978.
- 402 Carlson, T. N., Belles, J. E. and Gillies, R. R.: Transient water stress in a vegetation canopy:  
 403 simulations and measurements, *Remote Sens. Environ.*, 35, 175-186, 1991.
- 404 Chauhan, N.S., Miller, S. and Ardanuy, P.: Spaceborne soil moisture estimation at high  
 405 resolution: a microwave-optical/IR synergistic approach, *Int. J. Remote Sens.*, 22, 4599–  
 406 4646, 2003.
- 407 Clapp, R. B. and Hornberger, G. M.: Empirical equations for some soil hydraulic-properties,  
 408 *Water Resour. Res.*, 14, 601-604, 1978.
- 409 Foken, T., Wimmer, F., Mauder, M., Thomas, C. and Liebenthal C.: Some intercepts of energy  
 410 balance closure, *Atmos. Chem. Phys.*, 6, 4395-4402, 2006.
- 411 Giertz, S., Diekrüger, B. and Steup, G.: Physically-based modelling of hydrological processes in  
 412 a tropical headwater catchment (West Africa)–process representation and multi-criteria  
 413 validation, *Hydrol. Earth Syst. Sc.*, 10, 829-847, 2006.
- 414 Gillies, R. R., Carlson, T. N., Cui, J., Kustas, W. P., and Humes K.S.: Verification of the “triangle”  
 415 method for obtaining surface soil water content and energy fluxes from remote  
 416 measurements of the Normalized Difference Vegetation Index NDVI and surface radiant  
 417 temperature, *Int. J. Remote Sens.*, 18, 3145–3166, 1997.
- 418 Gillies, R. R.: A physically-based land use classification scheme using remote solar and thermal  
 419 infrared measurements suitable for describing urbanisation. PhD Thesis, University of  
 420 Newcastle, UK, 121pp, 1993.
- 421 Hollinger, D. & Richardson, A.: Uncertainty in eddy covariance measurements and its  
 422 application to physiological models, *Tree Physiol*, 25, 873-885, 2005.
- 423 Ireland, G., Volpi, M. & G.P., Petropoulos (2014): Semi-automated flooded area cartography  
 424 from EO single image analysis and machine learning: a case study from a Mediterranean  
 425 river flood. *Remote Sensing MDPI*, 7, 3372-3399.
- 426 Liu, Y., Hiyama, T. and Yamaguchi Y.: Scaling of land surface temperature using satellite data: A  
 427 case examination on ASTER and MODIS products over a heterogeneous terrain area, *Rem.*  
 428 *Sens. Envir.*, 105, 115-128, 2006.
- 429 Maayar, M., Price, D. T., Delire, C., Foley, J. A., Black, T. A. and Bessemoulin, P.: Validation of the  
 430 Integrated Biosphere Simulator over Canadian deciduous and coniferous boreal forest  
 431 stands, *J. Geophys. Res-Atmos.* (1984–2012), 106, 14339-14355, 2001.

- 432 Manabe, S.: Climate and the ocean circulation 1. The atmospheric circulation and the hydrology  
433 of the earth's surface, *Mon. Weather. Rev.*, 97, 739-774, 1969.
- 434 Marshall, M., Tu, K., Funk, C., Michaelsen, J., Williams, P., Williams, C. and Kutsch, W.: Improving  
435 operational land surface model canopy evapotranspiration in Africa using a direct remote  
436 sensing approach, *Hydrol. Earth Syst. Sc.*, 17, 1079-1091, 2013.
- 437 Mascart P, Taconet O, Pinty J.P. and Mehrez M., B.: Canopy resistance formulation and its effect  
438 in mesoscale models: a HAPEX perspective, *Agric. For. Meteorol.*, 54, 319–351, 1991.
- 439 Monin, A. S. and Obukhov, A.: Basic laws of turbulent mixing in the surface layer of the  
440 atmosphere, *Contrib. Geophys. Inst. Acad. Sci. USSR*, 151, 163-187, 1954.
- 441 Oncley, S.P., Foken, T., Vogt, R., Kohsiek, W., DeBruin, H. A. R, Berhofer, C., Christen, A., Van  
442 Gorsel, E., Grantz, D., Feigenwinter, C., Lehner, I., Liebenthal, C., Liu, H., Mauder, M., Pitacco,  
443 A., Ribeiro, L. and Weidinger, T.: The Energy Balance Experiment EBEX-2000. Part I:  
444 overview and energy balance. *Bound-Lay. Meteorol.*, 123, 1–28, 2007.
- 445 Papale, Dario; Reichstein, M; Aubinet, Marc; et al.: Towards a standardized processing of Net  
446 Ecosystem Exchange measured with eddy covariance technique: algorithms and  
447 uncertainty estimation. *Biogeosciences*. 3 (4), pp. 571–583, 2006.
- 448 Petropoulos G. P. and Carlson, T. N.: Retrievals of turbulent heat fluxes and soil moisture  
449 content by remote sensing, Chapter 19, in: *Advances in Environmental Remote Sensing:  
450 Sensors, Algorithms, and Applications*, Ed. Taylor and Francis, 556, 667–502, 2011.
- 451 Petropoulos G., Griffiths, H. M., and Ioannou-Katidis, P.: Sensitivity exploration of SimSphere  
452 land surface model towards its use for operational products development from Earth  
453 observation data, chapter 14, in: *Advancement in Remote Sensing for Environmental  
454 Applications*, edited by: Mukherjee, S., Gupta, M., Srivastava, P. K., and Islam, T., Springer,  
455 2013b.
- 456 Petropoulos, G. P., Griffiths, H. M., and Tarantola, S.: Towards Operational Products  
457 Development from Earth Observation: Exploration of SimSphere Land Surface Process  
458 Model Sensitivity using a GSA approach, 7th International Conference on Sensitivity  
459 Analysis of 25 Model Output, 1–4 July 2013, Nice, France, 2013a.
- 460 Petropoulos, G. P., Griffiths, H., and Tarantola, S.: Sensitivity analysis of the SimSphere SVAT  
461 model in the context of EO-based operational products development, *Environ. Modell.  
462 Softw.*, 49, 166–179, 2013c.
- 463 Petropoulos, G. P., Konstas, I., and Carlson, T. N.: Automation of SimSphere Land Surface Model  
464 Use as a Standalone Application and Integration with EO Data for Deriving Key Land  
465 Surface Parameters, European Geosciences Union, 7–12 April 2013, Vienna, Austria,  
466 2013d.
- 467 Petropoulos, G., Wooster, M. J., Kennedy, K., Carlson, T.N. and Scholze, M.: A global sensitivity  
468 analysis study of the 1d SimSphere SVAT model using the GEM SA software, *Ecol. Model.*,  
469 220, 2427-2440, 2009a.
- 470 Petropoulos, G., Carlson, T. and Wooster, M. J.: An Overview of the Use of the SimSphere Soil  
471 vegetation Atmospheric Transfer (SVAT) Model for the Study of Land Atmosphere  
472 Interactions, *Sensors*, 9, 4286-4308, 2009b.
- 473 Petropoulos, G.P., G. Ireland, S. Lamine, N. Ghilain, V. Anagnostopoulos, M.R. North, P.K.  
474 Srivastava & H. Georgopoulou: Evapotranspiration Estimates from SEVIRI to Support  
475 Sustainable Water Management. *Journal of Applied Earth Observation & Geoinformation*,  
476 49, 175-187, 2016.
- 477 Petropoulos, G.P., Griffiths, H.M., Carlson, T.N., Ioannou-Katidis., P. and Holt, T.: SimSphere  
478 Model Sensitivity Analysis Towards Establishing its Use for Deriving Key Parameters

479 Characterising Land Surface Interactions, *Geoscientific Model Development Discussions*, 7,  
480 1873-1887, 2014.

481 Petropoulos, G.P., North, M. R., Ireland, G., Srivastava, P.K., & D.V., Rendall: Quantifying the  
482 prediction accuracy of a 1-D SVAT model at a range of ecosystems in the USA and  
483 Australia: evidence towards its use as a tool to study Earth's system interactions.  
484 *Geoscientific Models Development*, 8, 3257-3284, 2015

485 Piles, M., Camps, A., Vall-Llossera, M., Corbella, I., Panciera, R., Rudiger, C., Kerr, Y. H. and  
486 Walker, J.: Downscaling SMOS-derived soil moisture using MODIS visible/infrared data,  
487 *IEEE Geosci. Remote S.*, 49, 3156-3166, 2011.

488 Piles, M., G.P. Petropoulos, G. Ireland & N. Sanchez: A Novel Method to Retrieve Soil Moisture at  
489 High Spatio-Temporal Resolution Based on the Synergy of SMOS and MSG SEVIRI  
490 observations. *Rem. Sens. Environ.*, 2016.

491 Prentice, I. C., Liang, X., Medlyn, B. E., and Wang, Y. P.: Reliable, robust and realistic: the three  
492 R's of next-generation land surface modelling, *Atmos. Chem. Phys.*, 14, 24811-24861,  
493 2014.

494 Ross, S. L. and Oke, T. R.: Tests of three urban energy balance models, *Bound-Lay.*  
495 *Meteorol.*, 44, 73-96, 1988.

496 Todhunter, P. E. and Terjung, W. H.: Intercomparison of three urban climate models, *Bound-*  
497 *Lay. Meteorol.*, 42, 181-205, 1988.

498 Verbeeck, H., Samson, R., Granier, A., Montpied, P. and Lemeur, R.: Multi-year model analysis of  
499 GPP in a temperate beech forest in France, *Ecol. Model.*, 210, 85-109, 2008.

500 Wilson, K., Goldstein, A., Falge, E., Aubinet, M., Baldocchi, D., Berbigier, P. and Verma, S.: Energy  
501 balance closure at FLUXNET sites, *Agric. For. Meteorol.*, 113, 223-243, 2002.

502

## List of Figures

- Figure 1: (Left) The three facets of SimSphere Architecture , (Right) different layers represented within SimSphere's vertical domain
- Figure 2: Overall methodology of SimSphere validation followed in this study
- Figure 3: Comparisons of predicted and observed a)  $R_{net}$  fluxes ( $Wm^{-2}$ ), b) LE fluxes ( $Wm^{-2}$ ), c) H fluxes ( $Wm^{-2}$ ), and d)  $T_{air}$  at 50m ( $^{\circ}C$ )

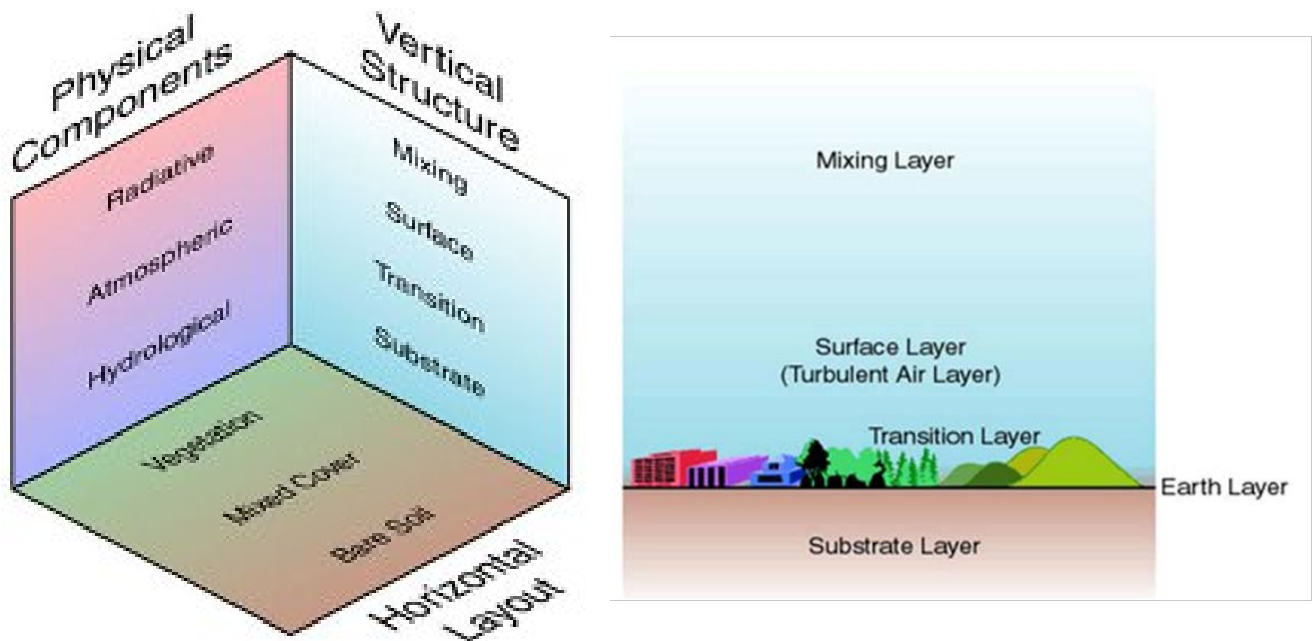


**Figure 1:** (Left) The three facets of SimSphere Architecture , (Right) different layers represented within SimSphere's vertical domain

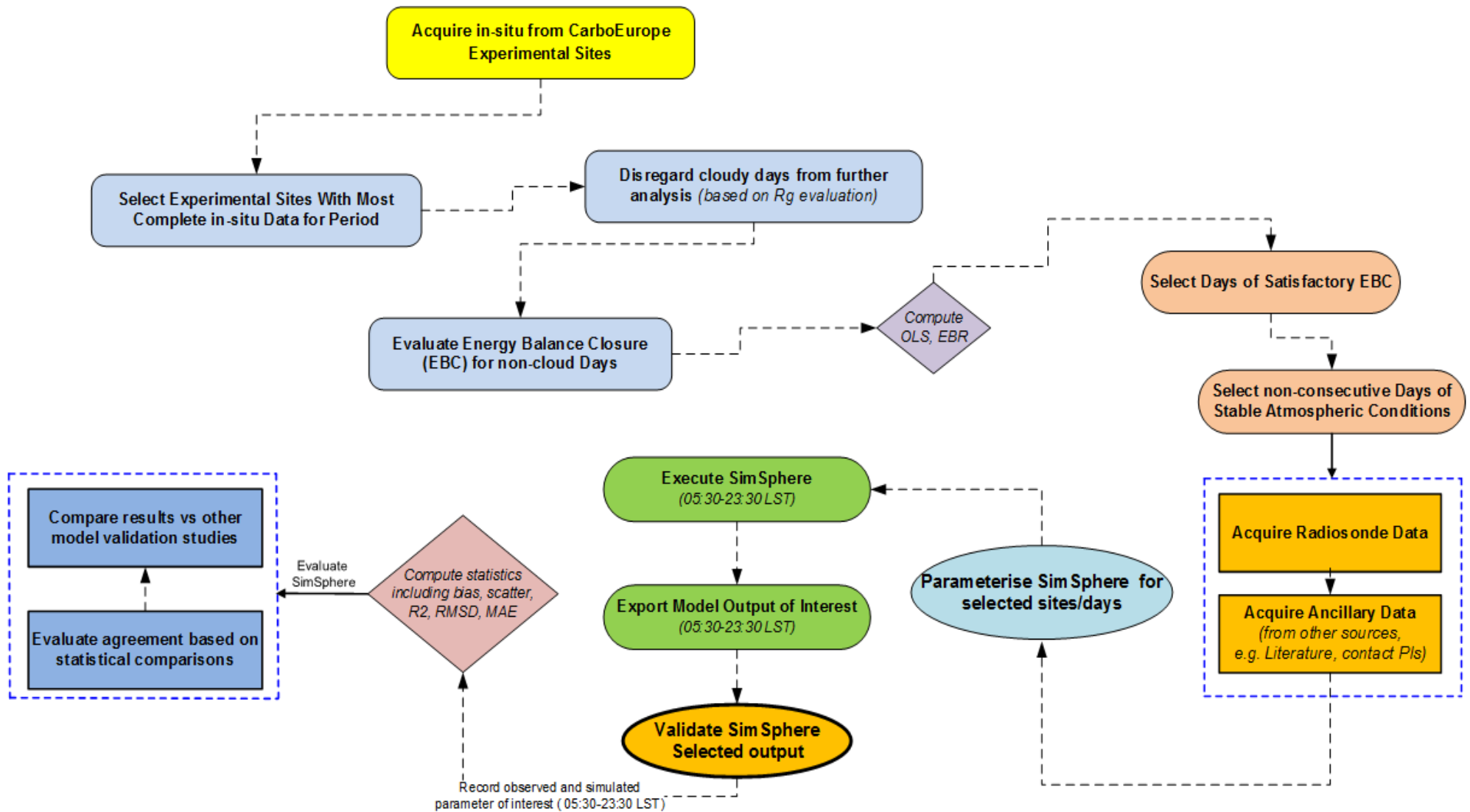
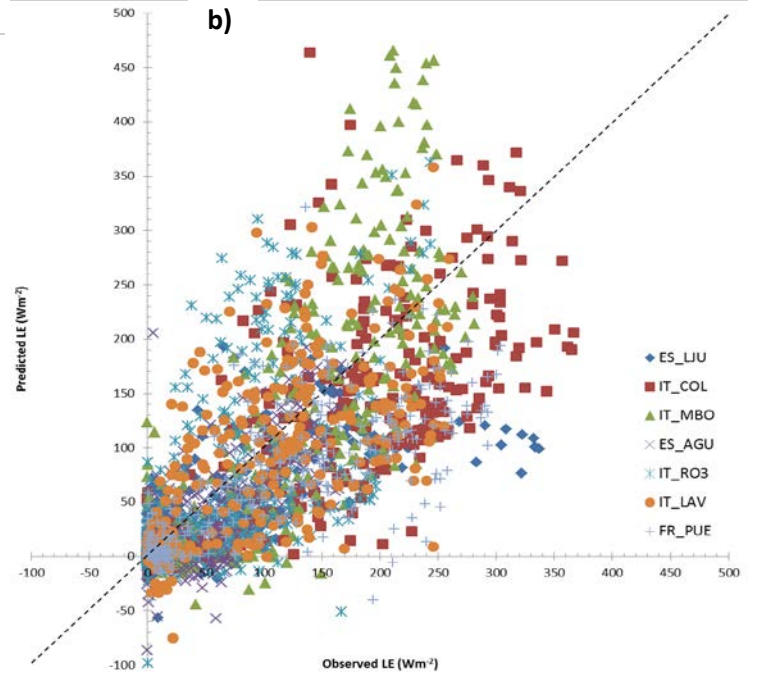
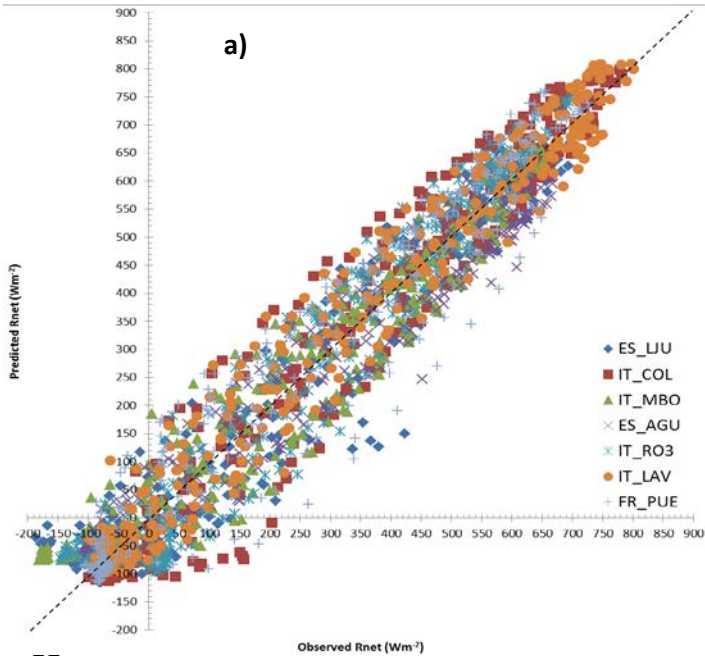
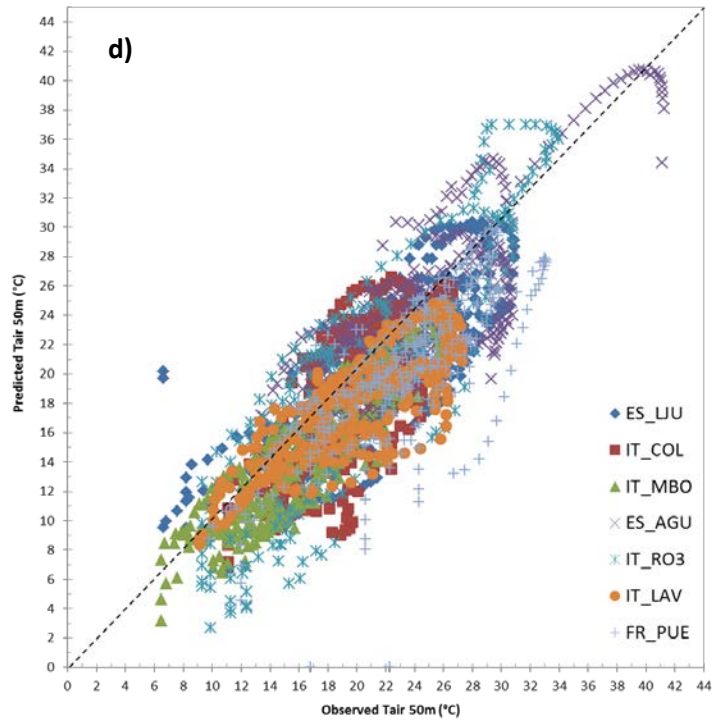
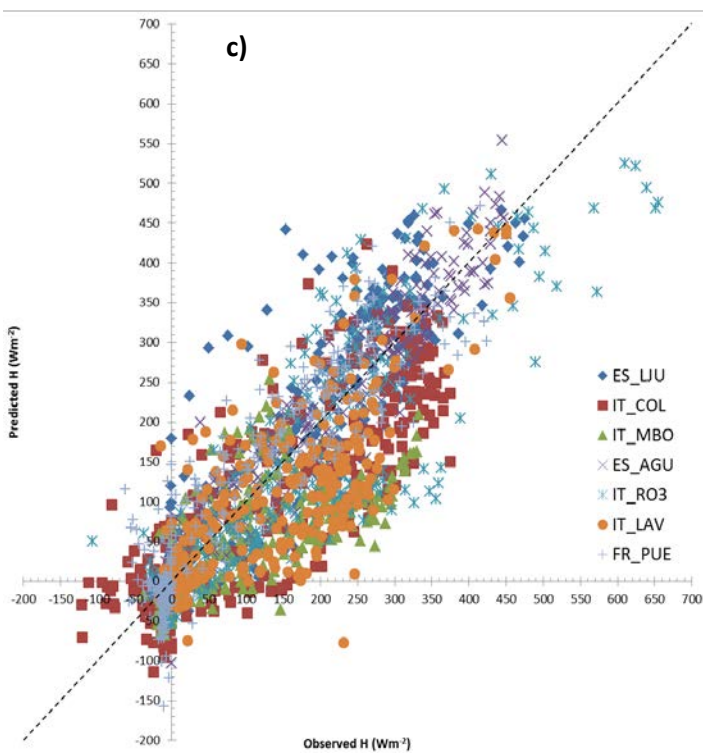


**Figure 2:** Overall methodology of SimSphere validation followed in this study

1



12



24 **Figure 3:** Comparisons of predicted and observed a)  $R_{net}$  fluxes ( $Wm^{-2}$ ), b) LE fluxes ( $Wm^{-2}$ ),  
 25 and c) H fluxes ( $Wm^{-2}$ )

26

**Table 1:** Summary of the main SimSphere inputs (top) and of its simulated outputs (bottom). The units are also provided in parentheses where applicable

NAME OF THE MODEL INPUT	PROCESS IN WHICH PARAMETER IS INVOLVED	MIN VALUE	MAX VALUE
Slope ( <i>degrees</i> )	TIME & LOCATION	0	45
Aspect ( <i>degrees</i> )	TIME & LOCATION	0	360
Station Height ( <i>meters</i> )	TIME & LOCATION	0	4.92
Fractional Vegetation Cover (%)	VEGETATION	0	100
LAI ( $m^2m^{-2}$ )	VEGETATION	0	10
Foliage emissivity ( <i>unitless</i> )	VEGETATION	0.951	0.990
[Ca] (external [CO <sub>2</sub> ] in the leaf) ( <i>ppmv</i> )	VEGETATION	250	710
[Ci] (internal [CO <sub>2</sub> ] in the leaf) ( <i>ppmv</i> )	VEGETATION	110	400
[O3] (ozone concentration in the air) ( <i>ppmv</i> )	VEGETATION	0.0	0.25
Vegetation height ( <i>meters</i> )	VEGETATION	0.021	20.0
Leaf width ( <i>meters</i> )	VEGETATION	0.012	1.0
Minimum Stomatal Resistance ( $sm^{-1}$ )	PLANT	10	500
Cuticle Resistance ( $sm^{-1}$ )	PLANT	200	2000
Critical leaf water potential ( <i>bar</i> )	PLANT	-30	-5
Critical solar parameter ( $Wm^{-2}$ )	PLANT	25	300
Stem resistance ( $sm^{-1}$ )	PLANT	0.011	0.150
Surface Moisture Availability ( <i>vol/vol</i> )	HYDROLOGICAL	0	1
Root Zone Moisture Availability ( <i>vol/vol</i> )	HYDROLOGICAL	0	1
Substrate Max. Volum. Water Content ( <i>vol/vol</i> )	HYDROLOGICAL	0.01	1
Substrate climatol. mean temperature ( $^{\circ}C$ )	SURFACE	20	30
Thermal inertia ( $Wm^{-2}K^{-1}$ )	SURFACE	3.5	30
Ground emissivity ( <i>unitless</i> )	SURFACE	0.951	0.980
Atmospheric Precipitable water ( <i>cm</i> )	METEOROLOGICAL	0.05	5
Surface roughness ( <i>meters</i> )	METEOROLOGICAL	0.02	2.0
Obstacle height ( <i>meters</i> )	METEOROLOGICAL	0.02	2.0
Fractional Cloud Cover (%)	METEOROLOGICAL	1	10
RKS (satur. thermal conduct. ( <i>Cosby et al., 1984</i> ))	SOIL	0	10
Cosby B ( <i>see Cosby et al., 1984</i> )	SOIL	2.0	12.0
THM (satur.vol. water cont.) ( <i>Cosby et al., 1984</i> )	SOIL	0.3	0.5
PSI (satur. water potential) ( <i>Cosby et al., 1984</i> )	SOIL	1	7
Wind direction ( <i>degrees</i> )	WIND SOUNDING PROFILE	0	360
Wind speed ( <i>knots</i> )	WIND SOUNDING PROFILE	---	---
Altitude ( <i>1000's feet</i> )	WIND SOUNDING PROFILE	---	---
Pressure ( <i>mBar</i> )	MOISTURE SOUNDING PROFILE	---	---
Temperature ( <i>Celsius</i> )	MOISTURE SOUNDING PROFILE	---	---
Temperature-Dewpoint Temperature ( <i>Celsius</i> )	MOISTURE SOUNDING PROFILE	---	---

## SimSphere Simulated Outputs

<b>Output Name</b>	<b>Units</b>		<b>Output Name</b>	<b>Units</b>
Air temperature at 1.3m	°C		Radiometric Temperature	°C
Air temperature at 50m	°C		Root Zone moisture Avail.	n/a
Air temperature at foliage	°C		Sensibel heat flux	Wm <sup>-2</sup>
Bowen ratio	n/a		Short-wave flux	Wm <sup>-2</sup>
[CO <sub>2</sub> ] on canopy	ppmv		Specific humidity at 1.3m	gKg <sup>-1</sup>
[CO <sub>2</sub> ] flux	micromolesm <sup>2</sup> s <sup>-1</sup>		Specific humidity at 50m	gKg <sup>-1</sup>
Epidermal water potential	Bars		Specific humidity at foliage	gKg <sup>-1</sup>
Global O <sub>3</sub> flux	Ugm <sup>-2</sup> s <sup>-1</sup>		Stomatal resistance	sm <sup>-1</sup>
Ground flux	Wm <sup>-2</sup>		Surface moisture availability	n/a
Ground water potential	bars		Vapor pressure deficit	Mbar
Latent Heat flux	Wm <sup>-2</sup>		Water Use Efficiency	n/a
Leaf water potential	bars		Wind at 10m	Kts
Net Radiation	Wm <sup>-2</sup>		Wind at 50m	Kts
[O <sub>3</sub> ] canopy	ppmv		Wind in foliage	Kts
[O <sub>3</sub> ] flux plant	Ugm <sup>-2</sup> s <sup>-1</sup>			

**Table 2:** *Some of the main characteristics of the selected CarboEurope sites used for SimSphere validation.*

Site Name	Site Abbreviation	County	Geographic Location	PFT	Ecosystem Type	Dominant Species	Elevation	Climate
Llano de los Juanes	Es_Lju	SPAIN	36.9266/-2.1521	OLI	Olive Plantation	Oleauropea, Macchia	1622m	Warm Temperate with dry, hot summer
Collelongo-SelvaPiana	It_Col	ITALY	41.8493/13.5881	DBF	Deciduous Broadleaf Forest	Fagussylvatica	1645m	Warm temperate fully humid with warm summer
Monte Modone	It_Mbo	ITALY	46.0296/11.0829	GRA	Grassland	Alpine meadow	1547m	Snow fully humid warm summer
Aguamarga	Es_Agu	SPAIN	36.8347/-2.2511	SHR	Annual Broadleaf Shrub	Sumac (Rhus), Toyon (Heteromeles) and Coffeeberry (Rhamnus) Species	195m	Arid Steppe Cold
Lavarone	It_Lav	ITALY	45.9553/11.2812	ENL	Evergreen Needle leaf forest	Pinussylvestris	1353m	Warm temperate fully humid with warm summer
Puechabon	Fr_Pue	FRANCE	43.7414/3.5958	EBF	Evergreen Broadleaf forest	Quercus ilex	211m	Warm Temperate with dry, hot summer
Roccarepampani	It_Ro3	ITALY	42.3753/11.9154	CRO	Cropland	Cereal Crop	320m	Warm Temperate with dry, hot summer

**Table 3:** An overview of the statistical measures implemented in this study to evaluate SimSphere's outputs against the corresponding in-situ data

Name	Description	Mathematical Definition
Bias/MBE	Bias (accuracy) or Mean Bias Error	$bias = \frac{1}{N} \sum_{i=1}^N (P_i - O_i)$
R <sup>2</sup>	Linear Correlation Coefficient of Determination of P <sub>1</sub> to O <sub>i</sub>	$R^2 = \left[ \frac{\sum_{i=1}^N (P_i - \bar{P})(O_i - \bar{O})}{\left[ \sum_{i=1}^N (O_i - \bar{O})^2 \sum_{i=1}^N (P_i - \bar{P})^2 \right]^{0.5}} \right]^2$
Scatter/MSE	Scatter (precision) or Mean Standard Deviation	$scatter = \frac{1}{(N-1)} \sum_{i=1}^N (P_i - O_i - \overline{(P_i - O_i)})^2$
RMSD	Root Mean Square Difference	$RMSD = \sqrt{bias^2 + scatter^2}$
MAE	Mean Absolute Error	$MAD = N^{-1} \sum_{i=1}^N  P_i - O_i $
NASH	Nash Sutcliffe Efficiency	$NASH = 1 - \frac{\sum_{i=1}^N (O_i - S_i)^2}{\sum_{i=1}^N (O_i - \bar{O})^2}$

**Table 4: An overview of  $R_{net}$  simulation accuracy**

Site	P F T	Day	Statistical Test					Site	P F T	Day	Statistical Test				
			Bias	Scatter	RMSD	MAE	NASH				Bias	Scatter	RMSD	MAE	NASH
ES_LJU	O L I	14/04/2011	-24.55	42.31	48.91	32.45	0.921	IT_RO3	C R O	09/04/2011	-8.20	85.76	86.16	76.40	0.912
		09/05/2011	-19.34	60.31	63.33	47.55	0.976			11/04/2011	-52.87	46.21	70.22	55.97	0.913
		24/06/2011	12.18	67.54	68.63	57.97	0.916			18/04/2011	13.74	80.88	82.03	72.17	0.990
		27/06/2011	6.06	66.98	67.25	47.26	0.978			21/04/2011	24.95	56.34	61.62	55.09	0.982
		19/07/2011	26.05	57.38	63.01	44.21	0.934			20/06/2011	-12.51	53.15	54.60	48.95	0.937
		28/07/2011	34.52	56.12	65.89	47.60	0.971			26/06/2011	-22.36	48.39	53.30	42.70	0.972
		04/08/2011	15.06	51.08	53.25	33.81	0.930			24/08/2011	13.94	54.53	56.28	41.84	0.961
		22/08/2011	8.26	57.55	58.14	47.33	0.899			28/08/2011	-8.98	59.95	60.62	51.20	0.899
		25/08/2011	10.23	59.03	59.91	49.44	0.978			09/09/2011	-19.92	67.62	70.49	62.77	0.897
		28/09/2011	-19.69	92.19	94.27	78.84	0.998			11/09/2011	2.40	68.15	68.19	55.23	0.971
		<b>Average</b>	<b>4.88</b>	<b>64.78</b>	<b>64.96</b>	<b>48.65</b>	<b>0.950</b>			<b>Average</b>	<b>-6.98</b>	<b>66.53</b>	<b>66.90</b>	<b>56.23</b>	<b>0.943</b>
IT_COL	D B F	26/06/2011	-29.91	67.82	74.12	52.94	0.969	IT_LAV	E N L	27/06/2011	-24.60	57.52	62.56	46.13	0.971
		08/07/2011	-23.15	46.34	51.80	41.84	0.978			03/07/2011	-60.69	39.12	72.21	63.35	0.986
		13/07/2011	-12.95	56.81	58.27	50.16	0.934			09/07/2011	-35.90	57.43	67.73	58.59	0.971
		18/07/2011	-23.69	54.99	59.87	48.72	0.978			11/08/2011	-16.51	31.22	35.32	30.06	0.998
		11/08/2011	-10.67	63.23	64.12	50.03	0.974			12/08/2011	-0.79	31.24	31.25	24.10	0.996
		23/08/2011	14.50	64.17	65.79	54.93	0.940			20/08/2011	3.59	31.32	31.53	21.85	0.975
		11/09/2011	40.85	53.96	67.67	47.63	0.899			21/08/2011	23.69	29.01	37.46	32.13	0.989
		15/09/2011	38.95	59.52	71.13	52.79	0.969			24/08/2011	47.45	25.99	54.10	47.45	0.990
		16/09/2011	18.84	70.23	72.71	50.39	0.999			09/09/2011	33.71	46.83	57.70	49.08	0.979
		17/09/2011	44.54	54.46	70.36	47.23	0.920			30/09/2011	58.84	78.66	98.26	78.02	0.954
		<b>Average</b>	<b>4.61</b>	<b>68.03</b>	<b>68.19</b>	<b>51.16</b>	<b>0.956</b>			<b>Average</b>	<b>-9.70</b>	<b>55.01</b>	<b>55.86</b>	<b>44.02</b>	<b>0.981</b>
IT_MBO	G R A	10/04/2011	-45.49	54.34	70.87	47.71	0.979	FR_PUE	E B F	06/04/2011	-48.91	48.89	69.15	52.63	0.978
		10/05/2011	-22.05	41.00	46.56	37.14	0.936			09/04/2011	-39.03	51.27	64.43	50.03	0.913
		25/06/2011	-11.70	21.39	24.38	18.92	0.901			16/04/2011	-57.09	45.67	73.11	57.57	0.932
		03/07/2011	-12.38	66.20	67.35	56.63	0.978			17/05/2011	-27.98	49.22	56.62	46.95	0.946
		24/08/2011	40.61	55.84	69.04	46.81	0.925			28/05/2011	-38.36	48.14	61.55	50.92	0.961
		25/08/2011	41.22	61.04	73.66	50.97	0.978			19/06/2011	-58.10	49.41	76.27	64.97	0.947
		13/09/2011	-23.86	80.95	84.39	78.38	0.963			08/07/2011	-27.62	38.41	47.31	37.66	0.975
		21/09/2011	-21.12	75.19	78.10	69.16	0.910			26/09/2011	49.90	44.96	67.17	49.90	0.963
		26/09/2011	-3.44	67.29	67.38	59.95	0.912			14/09/2011	60.09	48.58	77.27	60.09	0.978
		30/09/2011	-5.05	49.55	49.81	43.63	0.978			20/09/2011	47.71	62.85	78.91	51.51	0.938
		<b>Average</b>	<b>-6.33</b>	<b>65.07</b>	<b>65.38</b>	<b>50.93</b>	<b>0.946</b>			<b>Average</b>	<b>-15.99</b>	<b>66.60</b>	<b>68.49</b>	<b>52.47</b>	<b>0.953</b>
ES_AGU	S H R	07/04/2011	-49.42	23.11	54.55	49.42	0.978								
		27/04/2011	-62.87	26.14	68.09	62.87	0.963								
		08/05/2011	-41.11	19.67	45.58	41.11	0.974								
		14/05/2011	-14.87	34.17	37.26	33.38	0.954								
		23/05/2011	-24.01	24.79	34.51	31.38	0.960								
		13/07/2011	27.95	26.78	38.71	32.17	0.980								
		29/07/2011	52.86	64.52	83.40	68.43	0.979								
		14/08/2011	55.68	50.21	74.97	67.51	0.968								
		26/08/2011	59.11	52.30	78.92	70.46	0.989								
		07/09/2011	41.81	48.79	64.25	59.21	0.972								
		<b>Average</b>	<b>15.02</b>	<b>60.92</b>	<b>62.75</b>	<b>53.40</b>	<b>0.972</b>								
<b>ALL SITES</b>		<b>AVERAGE</b>	<b>-2.07</b>	<b>63.85</b>	<b>64.65</b>	<b>50.98</b>	<b>0.96</b>								

**Table 5: An overview of LE simulation accuracy**

Site	P F T	Day	Statistical Test					Site	P F T	Day	Statistical Test				
			Bias	Scatter	RMSD	MAE	NASH				Bias	Scatter	RMSD	MAE	NASH
ES_LJU	O L I	14/04/2011	13.10	43.69	45.62	34.00	0.987	IT_RO3	C R O	09/04/2011	-34.88	54.19	64.45	39.69	0.996
		09/05/2011	-8.48	37.57	38.51	26.45	0.993			11/04/2011	-39.35	43.02	58.30	41.49	0.997
		24/06/2011	42.62	62.22	75.42	63.34	0.977			18/04/2011	-17.47	21.90	28.02	20.97	0.998
		27/06/2011	46.98	59.15	75.53	60.96	0.968			21/04/2011	1.65	27.69	27.74	20.70	0.998
		19/07/2011	17.78	25.03	30.70	23.02	0.954			20/06/2011	51.85	54.15	74.97	55.86	0.954
		28/07/2011	26.35	23.88	35.57	30.00	0.961			26/06/2011	38.33	31.82	49.81	39.17	0.960
		04/08/2011	-13.97	24.09	27.85	21.57	0.966			24/08/2011	12.15	28.29	30.79	22.73	0.984
		22/08/2011	-3.40	38.77	38.92	28.53	0.987			28/08/2011	18.05	26.51	32.07	23.96	0.973
		25/08/2011	22.97	33.43	40.56	29.31	0.902			09/09/2011	46.93	45.17	65.14	47.73	0.972
		28/09/2011	22.00	28.76	36.21	26.91	0.903			11/09/2011	49.09	54.13	73.07	51.67	0.986
		<b>Average</b>	<b>21.09</b>	<b>51.49</b>	<b>55.64</b>	<b>37.22</b>	<b>0.983</b>			<b>Average</b>	<b>-0.87</b>	<b>68.48</b>	<b>68.48</b>	<b>47.51</b>	<b>0.982</b>
IT_COL	D B F	26/06/2011	26.53	30.72	40.59	30.21	0.915	IT_LAV	E N L	27/06/2011	-9.09	38.54	39.59	29.72	0.938
		08/07/2011	2.34	71.20	71.24	51.70	0.936			03/07/2011	23.40	41.88	47.97	38.47	0.973
		13/07/2011	33.33	53.23	62.81	47.75	0.976			09/07/2011	-16.39	55.28	57.66	41.60	0.912
		18/07/2011	35.85	70.07	78.71	62.73	0.935			11/08/2011	32.47	44.84	55.36	41.66	0.899
		11/08/2011	32.46	68.31	75.63	65.57	0.894			12/08/2011	29.70	67.43	73.68	59.10	0.937
		23/08/2011	-25.34	81.15	85.01	50.98	0.900			20/08/2011	31.48	80.52	86.45	63.16	0.936
		11/09/2011	56.10	42.26	70.23	56.10	0.986			21/08/2011	-12.13	45.44	47.04	33.46	0.938
		15/09/2011	60.69	49.42	78.27	61.47	0.984			24/08/2011	-21.87	57.06	61.11	46.97	0.989
		16/09/2011	50.25	47.72	69.30	53.45	0.987			09/09/2011	27.18	69.22	74.37	59.71	0.935
		17/09/2011	6.74	26.51	27.35	21.59	0.993			30/09/2011	9.78	40.27	55.69	48.69	0.913
		<b>Average</b>	<b>33.67</b>	<b>67.43</b>	<b>75.36</b>	<b>55.86</b>	<b>0.951</b>			<b>Average</b>	<b>8.47</b>	<b>58.32</b>	<b>58.93</b>	<b>41.39</b>	<b>0.937</b>
IT_MBO	G R A	10/04/2011	16.85	25.39	30.47	21.85	0.989	FR_PUE	E B F	06/04/2011	52.85	57.24	77.91	56.05	0.980
		10/05/2011	-35.35	42.72	55.45	40.52	0.913			09/04/2011	-17.44	39.39	43.08	25.79	0.996
		25/06/2011	6.87	59.93	60.33	49.33	0.976			16/04/2011	43.76	41.67	60.43	45.93	0.977
		03/07/2011	-26.51	73.75	78.37	56.20	0.911			17/05/2011	45.00	59.73	74.78	56.06	0.990
		24/08/2011	-19.29	51.79	55.27	37.79	0.978			28/05/2011	46.25	61.55	76.99	55.46	0.985
		25/08/2011	26.85	68.15	73.25	61.21	0.936			19/06/2011	28.64	43.41	52.01	39.13	0.993
		13/09/2011	-8.09	44.20	44.93	36.71	0.998			08/07/2011	22.05	38.52	44.38	33.47	0.983
		21/09/2011	14.93	53.34	55.39	34.19	0.936			26/09/2011	49.04	44.60	66.28	50.75	0.985
		26/09/2011	14.52	52.12	54.10	39.33	0.978			14/09/2011	62.28	39.97	74.00	62.28	0.954
		30/09/2011	26.21	37.65	45.88	33.52	0.980			20/09/2011	11.54	19.56	22.71	18.02	0.987
		<b>Average</b>	<b>-3.45</b>	<b>74.58</b>	<b>74.66</b>	<b>52.87</b>	<b>0.959</b>			<b>Average</b>	<b>37.56</b>	<b>57.77</b>	<b>68.91</b>	<b>47.46</b>	<b>0.988</b>
ES_AGU	S H R	07/04/2011	-20.76	30.09	36.55	25.02	0.990								
		27/04/2011	-21.86	29.03	36.34	28.04	0.994								
		08/05/2011	-9.68	21.12	23.23	16.54	0.996								
		14/05/2011	9.05	20.14	22.08	17.51	0.990								
		23/05/2011	10.84	25.10	27.35	19.64	0.986								
		13/07/2011	27.01	28.63	39.36	31.06	0.884								
		29/07/2011	34.47	25.94	43.14	34.81	0.754								
		14/08/2011	25.42	24.42	35.25	28.31	0.947								
		26/08/2011	28.00	52.61	59.60	40.41	0.975								
		07/09/2011	36.65	37.96	52.76	39.47	0.953								
		<b>Average</b>	<b>13.99</b>	<b>34.53</b>	<b>37.25</b>	<b>25.58</b>	<b>0.947</b>								
<b>ALL SITES</b>		<b>AVERAGE</b>	<b>15.78</b>	<b>58.94</b>	<b>62.75</b>	<b>43.98</b>	<b>0.964</b>								

**Table 6: An overview of  $H$  simulation accuracy**

Site	P F T	Day	Statistical Test					Site	P F T	Day	Statistical Test				
			Bias	Scatter	RMSD	MAE	NASH				Bias	Scatter	RMSD	MAE	NASH
ES_LJU	O L I	14/04/2011	-29.24	44.75	53.45	39.51	0.985	IT_RO3	C R O	09/04/2011	10.92	39.80	41.27	26.92	0.934
		09/05/2011	-11.76	32.57	34.63	30.29	0.963			11/04/2011	31.67	30.24	43.79	34.75	0.919
		24/06/2011	-47.07	39.11	61.20	48.54	0.945			18/04/2011	42.10	42.34	59.71	44.00	0.958
		27/06/2011	-28.81	38.98	48.47	37.58	0.948			21/04/2011	33.35	52.28	62.01	42.53	0.961
		19/07/2011	-27.46	38.74	47.48	35.77	0.978			20/06/2011	-9.57	73.29	73.91	52.42	0.958
		28/07/2011	-43.87	50.48	66.88	51.27	0.915			26/06/2011	17.25	89.42	91.07	70.44	0.983
		04/08/2011	18.95	38.42	42.84	31.95	0.934			24/08/2011	16.30	43.62	46.56	36.97	0.917
		22/08/2011	-3.39	51.14	51.25	39.75	0.964			28/08/2011	-17.29	48.32	51.32	30.11	0.913
		25/08/2011	17.21	52.08	54.85	44.13	0.964			09/09/2011	-15.89	39.23	42.32	28.03	0.978
		28/09/2011	13.23	41.60	43.65	29.29	0.978			11/09/2011	-22.61	61.45	65.48	44.20	0.928
		<b>Average</b>	<b>-17.17</b>	<b>60.22</b>	<b>62.62</b>	<b>43.97</b>	<b>0.957</b>			<b>Average</b>	<b>15.53</b>	<b>70.23</b>	<b>71.93</b>	<b>47.95</b>	<b>0.945</b>
IT_COL	D B F	26/06/2011	1.74	46.77	46.80	33.26	0.899	IT_LAV	E N L	27/06/2011	-22.70	68.75	72.40	51.93	0.968
		08/07/2011	18.13	64.78	67.27	51.57	0.924			03/07/2011	-35.97	64.90	74.20	54.32	0.974
		13/07/2011	9.77	44.49	45.55	41.51	0.970			09/07/2011	-25.35	48.49	54.72	40.30	0.913
		18/07/2011	12.29	57.20	58.50	51.31	0.941			11/08/2011	5.65	41.04	41.42	32.01	0.978
		11/08/2011	-3.40	37.51	37.66	29.44	0.991			12/08/2011	0.32	32.85	32.85	25.04	0.963
		23/08/2011	55.49	53.01	76.74	60.69	0.997			20/08/2011	7.77	56.67	57.20	38.05	0.918
		11/09/2011	32.16	37.20	49.17	36.64	0.969			21/08/2011	9.11	51.09	51.90	38.97	0.978
		15/09/2011	21.18	73.90	76.88	62.74	0.879			24/08/2011	18.93	56.46	59.55	46.52	0.899
		16/09/2011	23.20	43.50	49.30	41.64	0.969			09/09/2011	3.34	71.63	71.71	55.63	0.910
		17/09/2011	-0.51	59.69	59.69	45.19	0.914			30/09/2011	41.43	41.04	58.31	43.60	0.989
		<b>Average</b>	<b>14.72</b>	<b>58.78</b>	<b>60.59</b>	<b>46.84</b>	<b>0.945</b>			<b>Average</b>	<b>-6.72</b>	<b>56.95</b>	<b>57.34</b>	<b>39.18</b>	<b>0.949</b>
IT_MBO	G R A	10/04/2011	-29.74	51.93	59.84	48.15	0.910	FR_PUE	E B F	06/04/2011	-36.45	36.93	51.89	38.72	0.978
		10/05/2011	0.29	20.03	20.03	16.50	0.971			09/04/2011	-4.73	61.85	62.03	46.98	0.995
		25/06/2011	4.97	32.86	33.23	25.14	0.896			16/04/2011	-42.22	50.00	65.44	49.12	0.914
		03/07/2011	15.82	67.80	69.62	42.00	0.941			17/05/2011	-50.66	49.10	70.55	53.69	0.968
		24/08/2011	36.06	22.46	42.48	37.55	0.879			28/05/2011	-4.18	60.90	61.04	49.30	0.978
		25/08/2011	32.11	22.49	39.20	32.69	0.986			19/06/2011	-37.85	59.70	70.69	64.09	0.925
		13/09/2011	15.15	26.73	30.73	22.44	0.976			08/07/2011	-14.58	40.37	42.93	35.78	0.946
		21/09/2011	31.57	24.50	39.96	32.22	0.936			26/09/2011	11.57	31.31	33.38	26.11	0.917
		26/09/2011	16.48	13.24	21.14	17.15	0.914			14/09/2011	23.07	42.11	48.01	38.77	0.913
		30/09/2011	41.43	41.04	58.31	43.60	0.989			20/09/2011	-6.86	28.55	29.36	20.38	0.979
		<b>Average</b>	<b>16.41</b>	<b>40.97</b>	<b>44.13</b>	<b>31.74</b>	<b>0.940</b>			<b>Average</b>	<b>-16.29</b>	<b>52.98</b>	<b>55.43</b>	<b>42.29</b>	<b>0.951</b>
ES_AGU	S H R	07/04/2011	-1.09	30.30	30.32	25.05	0.991								
		27/04/2011	-17.07	24.53	29.89	24.17	0.930								
		08/05/2011	-8.29	29.72	30.85	22.23	0.978								
		14/05/2011	-10.76	24.77	27.00	22.46	0.915								
		23/05/2011	-30.75	33.29	45.32	33.51	0.997								
		13/07/2011	-27.78	33.14	43.24	31.19	0.937								
		29/07/2011	-4.41	37.58	37.84	28.45	0.914								
		14/08/2011	20.68	35.58	41.16	31.22	0.989								
		26/08/2011	8.19	47.52	48.22	34.04	0.937								
		07/09/2011	0.07	30.02	30.02	22.99	0.993								
		<b>Average</b>	<b>-7.01</b>	<b>34.80</b>	<b>35.50</b>	<b>25.03</b>	<b>0.958</b>								
<b>ALL SITES</b>		<b>AVERAGE</b>	<b>-0.08</b>	<b>53.56</b>	<b>55.36</b>	<b>39.57</b>	<b>0.95</b>								